

AMPLIFICATION FACTORS TO ESTIMATE INELASTIC DISPLACEMENT DEMANDS FOR THE DESIGN OF STRUCTURES IN THE NEAR FIELD

Jose I BAEZ¹ And Eduardo MIRANDA²

SUMMARY

The effects of rupture directivity at near-fault sites on the ratio of maximum inelastic displacement demand to maximum elastic displacement demand are investigated. Inelastic displacement ratios are computed for single-degree-of-freedom systems undergoing different levels of inelastic deformation when subjected to 82 earthquake ground motions recorded at distances closer than 15 km from the surface projection of the rupture. It is found that in addition to increments of linear elastic spectral ordinates in the long period spectral region previously identified by seismologists, forward directivity effects can affect the ratio of maximum inelastic displacement demand to maximum elastic displacement demand. Results indicate that inelastic displacement ratios computed from near-fault records are typically larger than those computed from distant records for periods between 0.1 and about 1.3s. Similarly, inelastic displacement ratios corresponding to fault-normal components are, in general, larger than those of fault-parallel components in the same spectral region. From various ground motions parameters investigated that may affect inelastic displacement ratios of structures located in the near field it is found that peak ground velocity and maximum incremental velocity are the most important ones. Results show that structures subjected to ground motions with large velocity pulses may experience maximum inelastic deformations larger than those subjected to ground motions that do not have these pulses, even if linear elastic ordinates in the short period spectral region are similar. Thus, it is concluded that modification of linear elastic design spectra alone may not be enough to adequately control maximum inelastic deformations in structures located near active faults.

INTRODUCTION

Some near-fault earthquake ground motions are characterised by having long duration acceleration pulses that give rise to unusually large velocity pulses. These pulses are the result of the earthquake rupture moving toward the site (forward rupture directivity). Furthermore, these pulses are typically much more pronounced on the horizontal component oriented perpendicular to the fault strike (fault normal). Directivity effects may occur not only on strike-slip faulting but also on dip-slip faulting including both normal and reverse faulting.

The study of theoretical dislocation models to understand the kinematics of near-field ground motions is by no means new [2]. However, after the 1994 Northridge and the 1995 Hyogo-Ken Nambu (Kobe) earthquakes this topic has gained particular recognition among seismologists. Recently, using empirical analyses of near-fault recordings and checked using broadband strong motion simulations, several proposals have been made to quantify these effects, sometimes referred to as “fling”, to modify existing empirical attenuation relationships to incorporate average rupture directivity effects [10] and more recently to incorporate normal fault forward directivity effects [1,11,12].

The significance of large velocity pulses encountered in near-fault ground motions on structural response was first pointed out by Bertero and Mahin after the 1971 San Fernando earthquake [4,8]. After the 1979 Imperial Valley earthquake Anderson and Bertero [2] identified the incremental velocity as an important parameter

¹ Graduate School of Engineering, National Autonomous University of Mexico, 04510 Mexico, jibj@servidor.unam.mx

² ERN Consulting Engineers, Calle Dos No. 2, Int. 2, 03240 Mexico, D.F. MEXICO, ermexico@compuserve.com.mx

affecting the maximum inelastic response of structures subjected to near-fault ground motions. More recently and as a result of the 1994 Northridge and the 1995 Hyogo-ken-Nambu (Kobe) earthquakes near-source factors have been introduced in the 1997 Uniform Building Code [13]. These factors range from 1.0 to 2.0 as a function of the source type and the closest distance to known seismic source. However, these new factors have been introduced based on limited data and studies and do not explicitly take into account the difference between the effects of near-fault ground motions on elastic and on inelastic structural response.

Other design recommendations have recently introduced factors that explicitly take into account the maximum inelastic to maximum elastic lateral displacement demand [3,6]. These factors permit the estimation of maximum inelastic displacements using the results of linear elastic analyses. The objective of this paper is to present the effects of near-fault earthquake ground motions on inelastic displacement ratios.

INELASTIC DISPLACEMENT RATIOS

The inelastic displacement ratio, C_μ , is defined as the maximum lateral inelastic displacement demand, $\Delta_{inelastic}$, divided by the maximum lateral elastic displacement demand, $\Delta_{elastic}$, on systems with the same mass and initial stiffness (i.e., same period of vibration) when subjected to a given earthquake ground motion, i.e.

$$C_\mu = \frac{\Delta_{inelastic}}{\Delta_{elastic}} \quad (1)$$

Thus, if information on this ratio is available, an estimation of the maximum inelastic displacement can be obtained from the maximum elastic displacement demand. In the study presented herein, inelastic displacement ratios were computed for SDOF systems having a viscous damping ratio of 5% and a nonlinear elasto-plastic hysteretic behaviour. Constant ductility inelastic displacement ratios were computed for six different levels of inelastic deformation corresponding to the following ductility ratios: 1.5, 2, 3, 4, 5 and 6. For each earthquake record and each target displacement ductility ratio, the inelastic displacement ratios were calculated by iteration on the lateral strength of the system for a set of 50 periods of vibration between 0.05 and 3.0 s. For more information on inelastic displacement ratios the reader is referred to Miranda [9].

NEAR-FAULT EARTHQUAKE GROUND MOTIONS CONSIDERED

A total of 82 acceleration time histories were considered in this study. Selected accelerations records have the following characteristics: (1) recorded at horizontal distances to the surface projection of the rupture not larger than 15 km; (2) recorded in earthquakes with strike-slip or dip-slip faulting mechanisms with surface wave magnitudes (M_s) larger than 5.6; (3) recorded at accelerographic stations where detailed information about the geographic, geological and geotechnical characteristics of the site is available; (4) recorded on sites with average shear wave velocities larger than 180 m/s; and (5) records in which both horizontal components have peak ground accelerations (PGA) larger than 200 cm/s² and peak ground velocities (PGV) larger than 20 cm/s.

Table 1 presents the ground motions considered in this study. They correspond to 9 North American earthquakes (8 from California and 1 from Canada). Table 1 includes the station name, the epicentral distance, horizontal distance from the recording site to the surface projection of the rupture, and maximum values of acceleration, velocity, displacement and incremental velocity.

PRESENTATION OF RESULTS

Figure 1 presents a comparison of mean inelastic displacement ratios computed in this study (82 near-fault records) to those computed from 218 earthquake ground motions recorded at stations more than 15 km away from the surface projection of the rupture. Mean inelastic displacement ratios on the right-hand side of figure 1 correspond to those computed by Miranda [9] but without including inelastic displacement ratios from 46 near-fault records. It can be seen that although in general they are similar, inelastic displacement ratios from near-fault records are larger, particularly for periods between 0.1 and 1.3s.

Table 1. Earthquake ground motions considered in this study.

Date	Earthquake Name	Magnitude (Ms)	Station Name	Distance 1 (km)	Distance 2 (km)	Comp.	PGA (cm/s ²)	PGV (cm/s)	PGD (cm)	Inc. Vel (cm/s)
9-Feb-71	San Fernando	6.6	Pacoima Dam	8.5	0.0	164	1148.1	113.2	37.66	143.09
						254	1054.9	57.7	10.82	97.30
6-Ago-79	Coyote Lake	5.7	Gilroy Array Station 6	9.7	1.2	230	413.7	43.8	9.34	70.70
						320	312.9	25.1	3.62	34.23
6-Ago-79	Coyote Lake	5.7	Gilroy # 4, San Ysidro School	12.6	3.7	270	229.0	25.1	2.95	38.56
						360	247.3	32.2	5.20	47.77
15-Oct-79	Imperial Valley	6.5	El Centro Array # 7, Imperial Valley College	29.4	0.6	140	326.8	44.7	24.31	64.25
						230	453.7	106.4	48.64	111.25
15-Oct-79	Imperial Valley	6.5	El Centro Array # 6, 551 Huston Road	29.8	1.3	140	368.7	62.2	29.18	62.18
						230	428.1	106.5	52.77	129.87
15-Oct-79	Imperial Valley	6.5	Bonds Corner	9.0	2.6	140	575.7	43.8	17.90	76.17
						230	770.4	47.3	18.12	83.56
15-Oct-79	Imperial Valley	6.5	El Centro Array # 8, Cruickshank Road	29.6	3.8	140	598.3	53.0	20.64	54.17
						230	457.4	49.4	38.53	50.75
15-Oct-79	Imperial Valley	6.5	El Centro Array # 5, James Road	30.5	4.0	140	517.2	44.1	42.19	51.95
						230	367.2	87.9	50.13	140.87
15-Oct-79	Imperial Valley	6.5	El Centro Array # 1, Dogwood Road	38.5	5.0	90	284.5	72.2	72.68	77.88
						180	371.9	51.2	60.31	87.07
15-Oct-79	Imperial Valley	6.5	El Centro Array # 4, Anderson Road	29.7	6.8	140	483.6	37.6	22.88	69.18
						230	349.7	77.8	48.56	118.40
15-Oct-79	Imperial Valley	6.5	Hotville, Post Office	22.7	7.5	225	246.2	44.2	29.48	58.29
						315	213.1	48.8	28.06	27.24
15-Oct-79	Imperial Valley	6.5	Brawley, Municipal Airport	46.3	8.5	225	162.2	35.3	36.92	46.43
						315	216.5	37.5	18.08	49.46
15-Oct-79	Imperial Valley	6.5	El Centro Array # 10, Community Hospital	29.8	8.5	50	168.2	45.1	30.07	76.72
						320	221.7	41.6	22.37	70.80
15-Oct-79	Imperial Valley	6.5	El Centro Array # 11, McCabe Union School	30.1	12.6	140	355.4	34.7	43.51	33.22
						230	374.5	39.3	16.38	43.55
15-Oct-79	Imperial Valley	6.5	El Centro Array # 3, Pine Union School	31.7	12.7	140	261.7	46.4	17.71	50.93
						230	218.1	37.3	23.52	25.22
23-Dic-85	Nahanni, Canada	6.9	Station # 1	7.0	0.0	10	1080.5	92.9	76.44	123.69
						280	1319.1	87.8	89.87	121.07
1-Oct-87	Whittier	6.1	Garvey Reservoir Abutment Bldg	11.3	3.4	60	367.1	30.8	8.59	56.97
						330	468.2	39.8	10.81	55.40
1-Oct-87	Whittier	6.1	Whittier, Whittier Narrows Dam (upstream)	11.1	5.1	33	294.0	39.4	7.34	58.09
						303	225.4	28.8	8.86	39.37
1-Oct-87	Whittier	6.1	Bell Los Angeles Bulk Mail Center	12.2	10.6	10	322.1	27.8	8.78	50.70
						280	436.9	71.2	13.59	109.89
1-Oct-87	Whittier	6.1	Vernon, Cmd Terminal	13.1	11.1	007	267.3	36.9	13.11	71.41
						277	239.9	40.6	12.43	66.41
17-Oct-89	Loma Prieta	7.0	Corralitos, Eureka Canyon Road	6.9	0.0	0	617.7	55.2	9.54	82.60
						90	469.4	47.5	11.53	83.17
17-Oct-89	Loma Prieta	7.0	Capitola Fire Station	9.7	8.6	0	462.9	36.1	11.02	57.48
						90	390.8	30.7	7.29	57.86
17-Oct-89	Loma Prieta	7.0	Gilroy 1, Gavillan Coll.	28.4	10.5	0	426.6	31.9	6.49	42.12
						90	433.6	33.8	6.32	54.18
17-Oct-89	Loma Prieta	7.0	Gilroy, Gavillan college Phys Sci Bldg	28.7	10.9	67	349.1	28.9	5.81	31.90
						337	310.0	23.0	4.78	32.02
17-Oct-89	Loma Prieta	7.0	Gilroy # 2, Hwy 101 Bolsa Road Motel	29.5	12.1	0	344.2	33.3	6.71	50.84
						90	316.3	39.2	10.89	60.30
17-Oct-89	Loma Prieta	7.0	Saratoga, Aloha Ave.	27.4	12.4	0	494.5	41.3	15.93	58.84
						90	316.2	43.6	27.98	38.09
17-Oct-89	Loma Prieta	7.0	Gilroy # 3, Sewage Treatment Plant	31.1	14.0	0	531.7	34.5	7.37	52.23
						90	362.0	43.8	14.32	44.91
25-Abr-92	Petrolia	7.0	Cape Mendocino	3.8	0.0	90	1019.4	40.5	14.80	63.82
						0	1468.3	126.1	36.07	142.28
25-Abr-92	Petrolia	7.0	Petrolia	5.4	5.0	90	649.4	89.5	30.58	131.49
						0	578.1	48.3	15.24	83.99
28-Jun-92	Landers	7.0	Lucerne Valley	42.0	1.0	0	611.7	32.1	89.91	31.70
						90	716.8	145.5	259.39	64.85
28-Jun-92	Landers	7.0	Joshua Tree, Fire Station	11.3	7.1	0	268.3	27.1	7.90	44.88
						90	278.4	42.7	15.73	62.55
17-Ene-94	Northridge	6.8	Los Angeles DAM	10.8	0.0	64	317.6	47.6	22.24	76.63
						334	419.1	76.4	20.30	100.10
17-Ene-94	Northridge	6.8	Rinaldi Receiving Station	9.9	0.0	319	471.0	80.3	21.88	119.41
						229	825.5	170.3	33.37	240.61
17-Ene-94	Northridge	6.8	Sepulveda Veterans Hospital	7.3	0.0	360	922.7	60.4	15.08	78.73
						270	738.2	61.1	11.44	120.77
17-Ene-94	Northridge	6.8	Sylmar Converter Station	12.3	0.0	322	569.2	107.5	33.75	196.76
						232	365.6	118.9	37.64	150.81
17-Ene-94	Northridge	6.8	Sylmar, County Hospital Parking Lot	15.8	2.0	90	592.6	76.9	15.22	107.22
						360	826.8	128.9	32.55	148.09
17-Ene-94	Northridge	6.8	White Oak Covenant Church, 17645 Saticoy St.	2.3	2.2	180	467.9	61.2	17.81	119.24
						90	357.0	31.1	9.23	53.61
17-Ene-94	Northridge	6.8	Arleta, Nordhoff Avenue Fire Station	9.9	4.0	90	337.3	40.4	8.88	67.59
						360	302.0	23.3	8.29	37.85
17-Ene-94	Northridge	6.8	Newhall, L.A. County Fire Station	20.2	5.0	90	571.6	74.8	17.60	102.78
						360	578.2	94.7	30.47	152.49
17-Ene-94	Northridge	6.8	Grace Community Church, 13248 Roscoe Blvd.	11.1	----	90	456.9	42.1	8.32	69.61
						0	279.9	23.2	5.13	38.21
17-Ene-94	Northridge	6.8	Knolls Elementary School, 6334 Katherine Road	13.0	----	90	503.4	44.6	5.24	69.82
						0	713.1	51.1	6.63	82.17

Distance 1: Epicentral distance.

Distance 2: Horizontal distance from the recording station to the surface projection of the rupture.

Inc. Vel: Maximum incremental velocity.

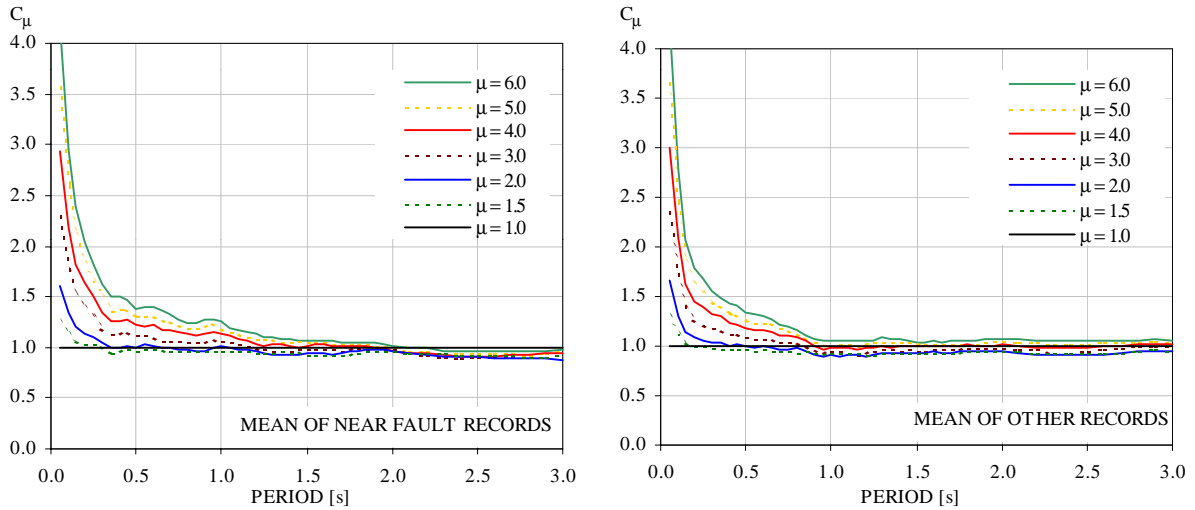


Figure 1. Comparison of mean inelastic displacement ratios computed from near-fault records to those from ground motions recorded more than 15 km away from the surface projection of the rupture.

Figure 2 presents the ratio of mean inelastic displacement ratios of the 82 near-fault records considered in this study to those computed from 218 earthquake ground motions recorded at stations more than 15 km away from the surface projection of the rupture. It can be seen that, in general, for periods of vibration smaller than about 1.3s inelastic displacement ratios from near-fault records are larger than those from distant records, whereas for periods longer than about 1.8s the opposite is true. The difference increases with increasing ductility ratios. Particularly important differences exist for periods around 0.2 and 0.95s.

The influence of several ground motion parameters on near-fault inelastic displacement ratios was investigated. The effect of maximum incremental velocity is shown in figure 3 where mean inelastic displacement ratios of near-fault records in three ranges of maximum incremental velocity are presented for displacement ductilities of three and six. Only near-fault records are included in this figure. It can be seen that inelastic displacement ratios from records with maximum incremental velocities larger than 55 cm/s are larger for periods of vibration between 0.1 and 0.8s, indicating that structures in the short period range close to active faults may experience larger inelastic displacement demands than those of more distant sites even if the elastic displacement demands were similar.

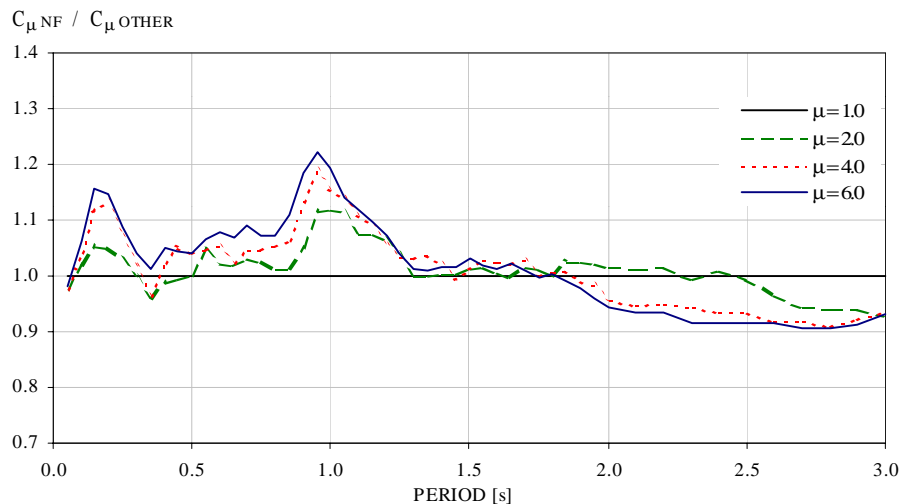


Figure 2. Ratio of mean inelastic displacement ratios of near-fault motions to those of distant sites.

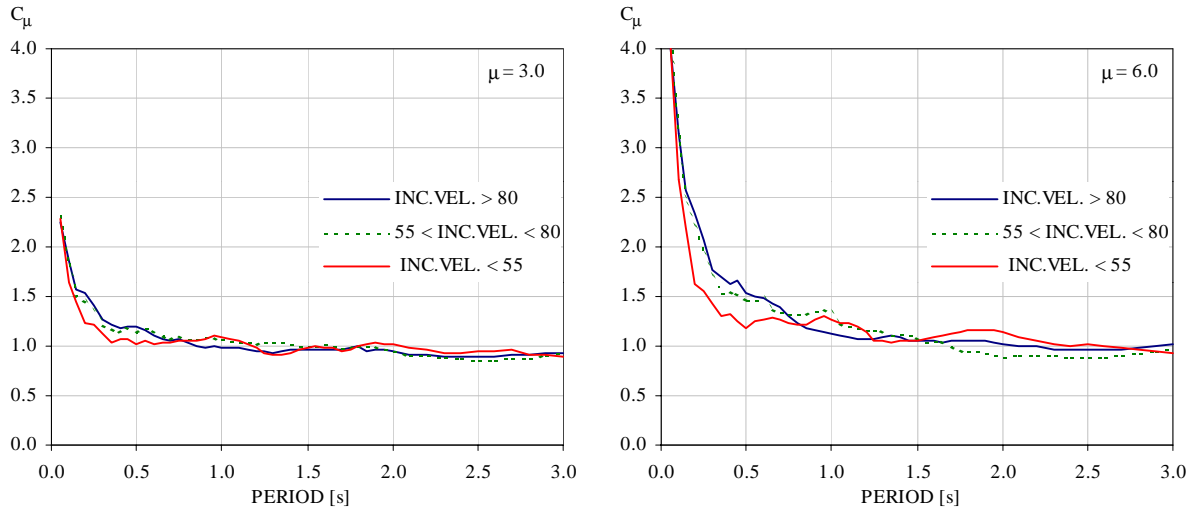


Figure 3. Effect of maximum incremental velocity on mean inelastic displacement ratios of near-fault earthquake ground motions.

Figure 4 shows the ratio of mean inelastic displacement ratios from 28 near-fault records with maximum incremental velocities higher than 80 cm/s to mean inelastic displacement ratios computed from 218 distant records. It can be seen that mean inelastic ratios from this group of 28 near-fault records are larger than those of distant records for periods smaller than 1.3s. For periods around 0.2s and high levels of ductility ($\mu \geq 4$) the inelastic displacement ratios from near-fault records with incremental velocities larger than 80 cm/s can be *on average* 1.3 times larger than those from distant records.

The effect of peak ground velocity (PGV) on mean inelastic displacement records of near-fault records is shown in figure 5. It can be seen that the effect of PGV is similar to that of the maximum incremental velocity. In this case near-fault ground motions with PGVs higher than 40 cm/s are larger for periods between 0.1 and 0.9s. Figure 6 shows the ratio of mean inelastic displacement ratios from 30 near-fault records with maximum ground velocities higher than 50 cm/s to mean inelastic displacement ratios computed from 218 distant records. It can be seen that mean inelastic ratios from this group of 30 near-fault records are larger than those of distant records for periods between 0.1 and 1.8s. In this period range and for ductilities of four or higher inelastic displacement ratios from near-fault records with PGVs larger than 50 cm/s are *on average* 5 to 30% higher than those from distant records.

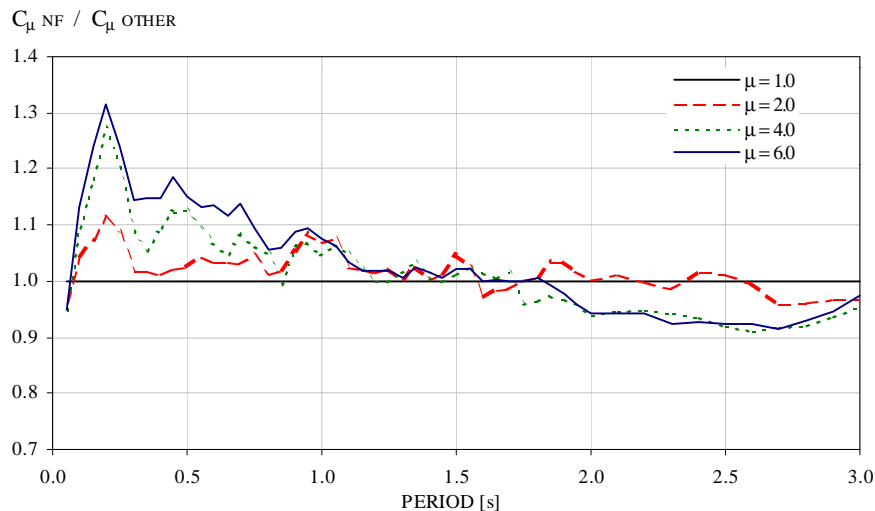


Figure 4. Ratio of mean inelastic displacement ratios from 28 near-fault records with maximum incremental velocity higher than 80 cm/s to those from 218 distant records.

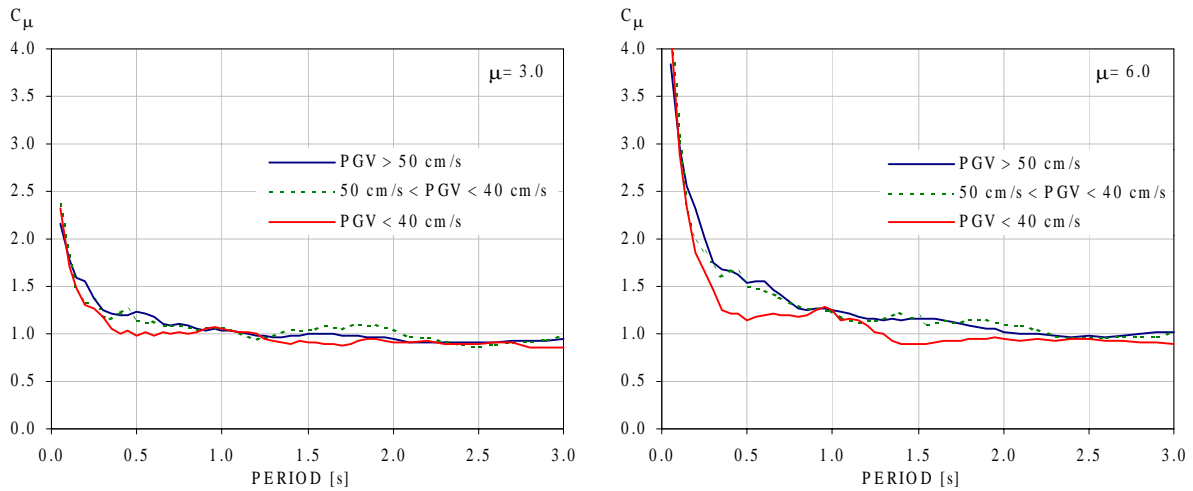


Figure 5. Effect of peak ground velocity on mean inelastic displacement ratios of near-fault earthquake ground motions.

As mentioned in the introduction, rupture directivity effects are particularly pronounced in the direction normal to the fault. Figure 7 shows a comparison of inelastic displacement ratios for horizontal components recorded at the Rinaldi Receiving Station. This recording station, operated by the Los Angeles Department of Water and Power, is located 10 km to the Northeast of the epicentre and on the surface projection of the rupture plane. This recording station measured a peak horizontal acceleration of 0.84g in the S49W component during the 1994 Northridge earthquake. The focal mechanism of the mainshock had one nodal plane striking $N75\pm 10^\circ W$. However, other determinations of the mainshock focal mechanism based on teleseismic and regional broadband waveforms show a more northerly strike of $N50-60^\circ W$. Thus, the S49W component, which recorded a PGV of 170.3 cm/s, is nearly normal to the fault plane whereas the N41W component, which recorded a PGV of 80.3 cm/s, is approximately parallel to the fault. The ratio of strong to weak recorded PGVs at this station is 2.12. Similarly, the maximum incremental velocity (MIV) in the strong component is 240.6 cm/s and 119.4 cm/s in the weak component. The ratio of MIVs in the strong to weak components is 2.01. It can be seen that for periods between 0.1 and 1.4s inelastic displacement ratios for the strong (nearly fault normal) component are larger than those of the weak (nearly fault parallel) component. The differences increase with increasing ductility ratios. For a ductility ratio of three the inelastic displacement ratio corresponding to a period of 0.35s of the strong component is 24% larger than that of the weak component. For a ductility ratio of six the inelastic displacement ratios corresponding to periods of vibration of 0.25s and 0.6s are more than 40% larger in the strong component than in the weak component.

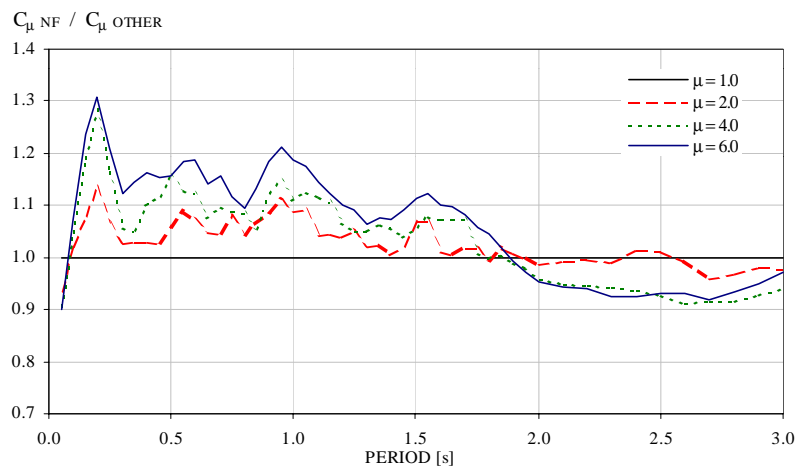


Figure 6. - Mean inelastic displacement ratios for maximum peak ground velocity higher than 50 cm/s normalised by mean inelastic displacement ratios for other sites.

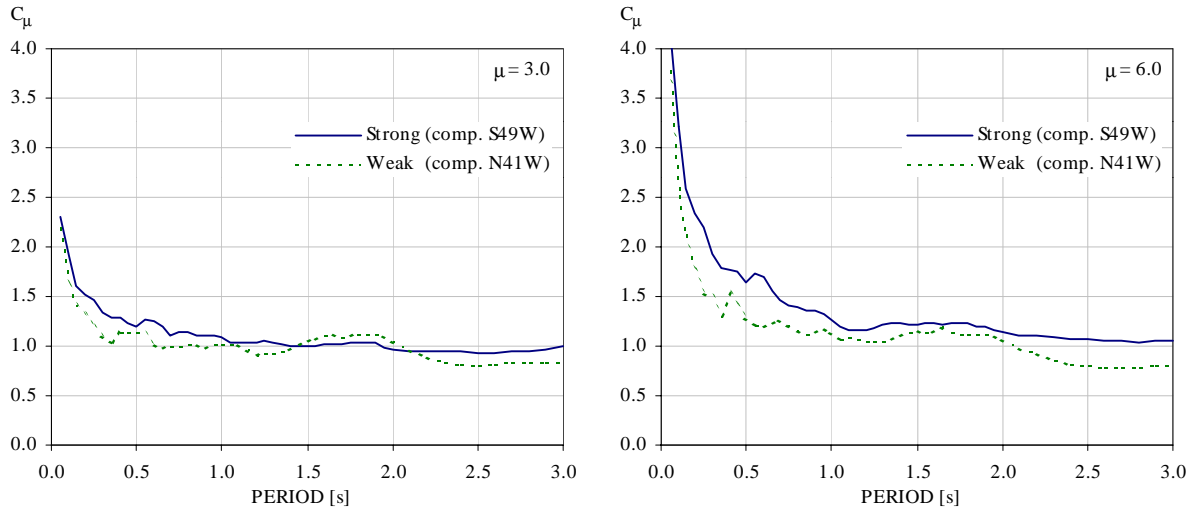


Figure 7. Inelastic displacement ratios for the weak and strong components of the ground motion recorded at the Rinaldi receiving station during the 1994 Northridge earthquake.

Figure 8 shows mean inelastic displacement ratios from pairs of horizontal motions obtained at 20 near-fault recording stations (40 records). On the left-hand side are mean inelastic displacement ratios from the weak components (those with the smaller maximum incremental velocity) and on the right-hand side mean inelastic displacement from the strong components are shown. It can be seen that for periods between 0.1 s and about 1.3s mean inelastic displacement ratios corresponding to the strong components are larger than those corresponding to the weak components.

It is important to notice that in all figures for extremely short periods (i.e., periods less than 0.1s) differences are very small on mean inelastic displacement ratios because as shown by Miranda [9], regardless of near-fault effects (distance to the surface projection of the rupture, peak ground velocity, maximum incremental velocity and orientation relative to the fault plane), inelastic displacement ratios tends to be equal to the displacement ductility ratio as $T \rightarrow 0$.

Although not shown here, because of space limitations, the effect of peak ground acceleration, peak ground displacement and epicentral distance were also investigated and found to have a much smaller effect on inelastic displacement ratios computed from near-fault records than the effect of the other parameters whose results are presented in this paper.

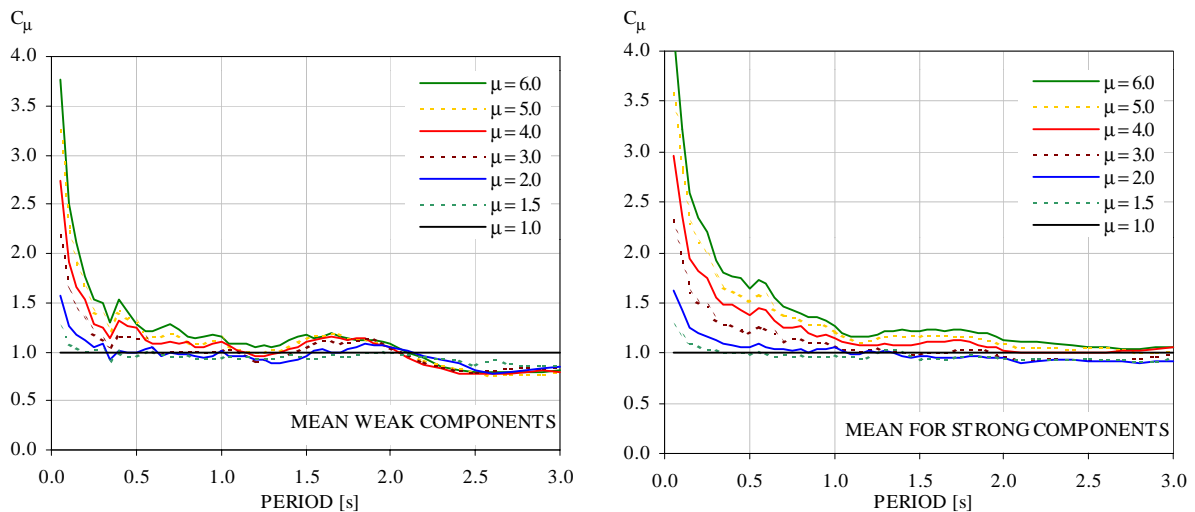


Figure 8. Mean inelastic displacement ratios for weak and strong components recorded at 20 stations.

CONCLUSIONS

The effect of rupture directivity at near-fault sites on inelastic displacement ratios was investigated. It is found that the inelastic structural response is very sensitive to the presence of long duration acceleration pulses that produce large inelastic excursions. Seismologists have pointed out that near-fault records affected by forward directivity rupture effects can have an important influence on the maximum *elastic* response of long period structures (periods longer than about 0.8s) [1, 10, 11, 12]. However, it is shown here that in addition to those increments in spectral ordinates for long periods, forward directivity effects can affect the ratio of maximum inelastic displacement demand to maximum elastic displacement demand. Inelastic displacement ratios computed from near-fault records are typically larger than those computed from distant records for periods between 0.1 and about 1.3s. Thus, modification of linear elastic design spectra alone, as done in the 1997 UBC [13], may not be enough to adequately control maximum inelastic deformations in structures in the near field.

Inelastic displacement ratios corresponding to fault-normal components are, in general, larger than those of fault parallel components for periods between 0.1 and about 1.3s. From various parameters that may affect mean ratios of maximum inelastic displacement demand to maximum elastic displacement demand for structures located near active faults it was found that peak ground velocity and maximum incremental velocity are the most important ones.

REFERENCES

1. Abrahamson, N.A. (1998), "Seismological aspects of near-fault ground motions", *Proc. of the 5th Caltrans Seismic Research Workshop*, California Department of Transportation, Sacramento, California.
2. Anderson, J.C., and Bertero, V.V. (1987), "Uncertainties in establishing design earthquakes", *Journal of Structural Engineering*, Vol.113, No.8, pp. 1709-1724.
3. Applied Technology Council (1996), "Improved seismic design criteria for California bridges: provisional recommendations," *Report No. ATC-32*, Redwood City, California.
4. Bertero, V.V., Mahin, S.A., and Herrera, R.A. (1977), "Problems in prescribing reliable design earthquakes", *Proceedings, 6th World Conference on Earthquake Engineering*, New Delhi, India, Vol. 2, pp. 1741-1746.
5. Boore, D.M., and Zoback, M.D. (1974), "Near-field motions from kinematic models of propagating faults," *Bulletin of the Seismological Society of America*, Vol. 64, No. 2, pp. 321-342.
6. Federal Emergency Management Agency (FEMA) (1997), "NEHRP guidelines for the seismic rehabilitation of buildings, Reports FEMA 273 (Guidelines) and 274 (Commentary), Washington, D.C.
7. Federal Emergency Management Agency (FEMA) (1997), "NEHRP recommended provisions for the seismic regulations for new buildings and other structures," *Report FEMA No. 302*, Washington, D.C.
8. Mahin, S.A., Bertero, V.V., Chopra, A.K., and Collins, R.G. (1976), "Response of the Olive View hospital main building during the San Fernando earthquake", *Report No. UCB/EERC-76/22*, Earthquake Engineering Research Center, University of California at Berkeley, Berkeley, California.
9. Miranda, E. (2000), "Inelastic displacement ratios for displacement-based earthquake resistant design," *Proc. 12th World Conference on Earthquake Engineering*, Auckland, New Zealand.
10. Somerville, P.G., Smith, N.F. Graves, R.W. and Abrahamson, N.A., (1995), "Representation of near-fault rupture directivity effects in design ground motions, and application to Caltrans bridges," *Proc. National Seismic Conf. on Bridges and Highways*, San Diego, California.
11. Somerville, P.G., and Smith, N.F. (1996), "Accounting for near-fault rupture directivity effects in the development of design ground motions", *Proc. 11th World Conference on Earthquake Engineering*, Acapulco, Mexico, Paper No. 711.
12. Somerville, P.G., Saikia, C.K., Wald, D.J., and Graves, R.W., (1996), "Implications of the Northridge earthquake for strong ground motions from thrust faults", *Bulletin Seismological Society of America*, Vol.86, Suppl., 1, Part B, pp. S115-S125.
13. Uniform Building Code (1997), Int. Conf. of Bldg. Officials, Whittier, California.